ImmunoTargets and Therapy

Dovepress
Taylor & Francis Group

Open Access Full Text Article

ORIGINAL RESEARCH

Anti-CD24 Antibody Plus Liposomal Doxorubicin for the Management of Residual Cancers After Incomplete Radiofrequency Ablation

Jiayun Liu[1–3,*], Bo Sun[1–3,*], Jing Li[1–3,*], Xiaocui Liu[1–3], Guilin Zhang[1–3], Ziqiao Lei[1–3], Chuansheng Zheng[1–3], Xuefeng Kan[1–3]

[1]Department of Radiology, Union Hospital, Tongji Medical College, Huazhong University of Science and Technology, Wuhan, 430022, People's Republic of China; [2]Hubei Provincial Clinical Research Center for Precision Radiology & Interventional Medicine, Wuhan, 430022, People's Republic of China; [3]Hubei Province Key Laboratory of Molecular Imaging, Wuhan, 430022, People's Republic of China

*These authors contributed equally to this work

Correspondence: Xuefeng Kan; Chuansheng Zheng, Department of Radiology, Union Hospital, Tongji Medical College, Huazhong University of Science and Technology, Wuhan, 430022, People's Republic of China, Email xkliulang1314@163.com; hqzcsxh@sina.com

Background: Achieving a complete radiofrequency ablation (RFA) for a solid malignant tumor of large size or at high-risk locations is challenging. A slow release of doxorubicin by liposomal doxorubicin (L-Dox) in solid tumors can selectively suppress the immune suppressive cells. In this study, the feasibility of using anti-CD24 antibody plus L-Dox was explored to inhibit residual cancers after incomplete RFA (iRFA) of hepatocellular carcinoma (HCC), with an attempt to reduce the tumor recurrences post-RFA.

Methods: The expressions of CD24 protein and sialic-acid-binding lg-like lectin 10 (Siglec-10) in residual cancers after iRFA of human HCC were evaluated. The mice orthotopic HCC models were treated by (1) pseudo iRFA: the ablation electrode was only put in the live tumor but without ablation treatment; (2) iRFA: the tumors only received iRFA treatment; (3) iRFA+anti-CD24 antibody; (4) iRFA+L-Dox; (5) iRFA+anti-CD24 antibody+L-Dox. The treatment effects and the immune microenvironment of treated tumors in each group were assessed and compared.

Results: The CD24 protein and Siglec-10 were highly expressed in the residual cancers ($p<0.001$). The iRFA+anti-CD24 antibody +L-Dox group had the smallest tumor size and the longest survival time ($p<0.001$). The anti-CD24 antibody in combination with L-Dox significantly decreased the expressions of CD24 and Siglec-10, significantly promoted the polarization of M2-like tumor-associated macrophages (TAMs) towards M1-like TAMs, significantly reduced the regulatory T cells and myeloid-derived suppressor cells, and significantly increased the infiltrations of natural killer cells and functional $CD8^+$T cells into residual cancers.

Conclusion: The combined therapy of anti-CD24 antibody with L-Dox could significantly improve the suppressive tumor immune microenvironment and result in a strong tumor-killing immunity in residual cancers, which significantly inhibited the residual cancers after iRFA of HCC. These findings may lead to a new strategy of enhancing the curative efficacy of RFA for large-sized HCC or HCC at high-risk locations.

Keywords: radiofrequency ablation, hepatocellular carcinoma, residual tumors, cd24 protein, liposomal doxorubicin

Introduction

Hepatocellular carcinoma (HCC) is the sixth most common malignancy, and the third leading cause of cancer death worldwide.[1] While radiofrequency ablation (RFA) is extensively employed for treating early-stage HCC, renal cell carcinoma, and non-small cell lung cancer,[2–4] incidence of tumor recurrence remains high after RFA, especially with large size tumors (>3 cm) or tumor at high-risk locations, such as tumors adjacent to large blood vessels, gallbladder, or diaphragm.[5,6] Furthermore, it has been reported that incomplete RFA (iRFA) of malignant solid tumors might increase invasiveness and metastasis of residual tumors.[7–9] Therefore, an effective treatment strategy to address this challenge is urgently needed.

Received: 29 May 2025
Accepted: 6 September 2025
Published: 18 September 2025

RFA of malignant solid tumors can result in a release of tumor-associated antigens, which could elicit an anti-tumor immune response.[10–12] Nonetheless, this immune antitumor effect does not always suffice to inhibit the residual tumors due to a high tumor-immunosuppressive microenvironment with massive immunosuppressive cells and fewer cytotoxic T cells in residual tumors.[13–16] Therefore, reprogramming a strong anti-tumor immune microenvironment in residual tumors may help decrease the recurrence of malignant solid tumors after RFA.

Prior studies[17–19] showed that CD24 protein was relatively highly expressed in HCC, ovarian cancer, and breast cancer, and the tumor-expressed CD24 protein could promote tumor immune evasion by interacting with sialic-acid-binding lg-like lectin 10 (Siglec-10), which was highly expressed in tumor-associated macrophages (TAMs).[19] TAMs are one of the most abundant immune cells that infiltrate the tumor microenvironment, and present at all stages of liver cancer progression.[20] When CD24 on tumor cells combines with Siglec-10 on immune cells, it causes the signal cascade of immune cell inhibition, which is mediated by SHP-1/SHP-2.[21] These could facilitate the polarization of M1-like TAMs towards M2-like TAMs, and thus promoting tumor occurrence, progression, and resistance to some chemotherapies.[22–24] Given these, CD24 is seen as a promising immune target for managing malignant tumors.

Liposomes are vesicles made up of a hydrophilic core and a lipophilic bilayer, which provides perfect opportunity for their application as a transport vehicle for various therapeutic agents.[25] Intratumoral injection of liposomal doxorubicin (L-Dox) allows doxorubicin to be released at a slow speed and on long-term basis, thereby resulting in doxorubicin accumulation and penetration in tumors, and reducing the systemic toxic side effects. Currently, the research effort is increasingly directed at a novel strategy that uses the low-to-medium dose doxorubicin at short repeating intervals to stimulate an anti-tumor immune microenvironment via emitting antigens and damage-associated molecular patterns (DAMPs),[26] and selectively inhibit the suppressive immune cells, such as M2-like TAMs, and myeloid-derived suppressor cells (MDSCs), regulatory T cells (Tregs).[14,27,28] Some studies[29–31] showed that doxorubicin could decrease the abundance of total TAMs in many cancers. Meanwhile, L-Dox could enhance immunological molecule expression on the tumor membrane, and directly destroy tumor cells by inhibiting the synthesis of DNA in tumor cells.[27] So, injection of L-Dox into residual tumors after iRFA could directly kill some tumor cells by inducing an immunogenic cell death, and thereby improve the suppressive tumor immune microenvironment. Recent studies[14,28] showed that the combination of L-Dox with pembrolizumab (anti-PD-1) or oncolytic peptide LTX-315 achieved a good anti-tumor effect. Given these reasons, the present study combined an anti-CD24 antibody with L-Dox to enhance the effect of RFA on HCC, with an aim to reduce the tumor recurrence post RFA and improve the patients' long-term survival.

Materials and Methods

Study Design

This study consisted of three phases: (1) in-vitro analyses the expression of CD24 protein and Siglec-10 in residual human HCC samples after iRFA; (2) in-vitro exploration of the effect of radiofrequency hyperthermia (RFH) plus knocking-out of CD24 on hepa1-6 cells; (3) in-vivo assessment of the effect of iRFA plus knocking-out of CD24 on orthotopic hepa1-6 tumor cells, and the feasibility of using anti-CD24 antibody in combination with L-Dox for removal of residual tumors after iRFA of HCC.

Cell Lines, Cell Culture, and Animals

The hepa1-6 cell line was obtained from Chinese Academy of Sciences, Shanghai, China. The cells were tested by a short tandem repeat analysis and were validated to be free of mycoplasma.

The green fluorescent protein (GFP)-positive hepa1-6 cells were created by transfecting GFP gene into hepa1-6 cells. The CD24 knocked-out hepa1-6 cells (CD24-KO-hepa1-6 cells) and CD24 knocked-out GFP-positive hepa1-6 cells were obtained by electroporating cells with recombinant CRISPR/Cas9 ribonucleoprotein (RNP). Briefly, CRISPR/Cas9 guide RNA molecules (Synthego, California) that targeted at mouse Cd24a were assembled with Cas9-3NLS nuclease (IDT) via incubating at 37°C for 45 minutes to form Cas9/RNP. Then the hepa1-6 cells (2×10^6) or GFP-positive hepa1-6 cells were combined with the corresponding complexed Cas9/RNP and electroporated with the Lonza Nucleofector IIb and Kit V (VCA-1003). After 48 hours of culture, the genetically modified cells were harvested and purified through at least

three successive rounds of fluorescence-activated sorting (FACS). The sequence of the guide RNA molecules is Cd24a sgRNA (AUAUUCUGGUUACCGGGAAA). These HCC cells were cultured in Dulbecco's Modified Eagle Medium (DMEM) (Gibco), supplemented with 10% fetal bovine serum (Gibco), and maintained in an incubator at 37°C with 5% CO2.

The C57BL/6 mice (male, 6–8 weeks old, Changsheng Biotechnology Co., Ltd, Liaoning, China) were used in the animal experiments of this study, which was approved by the Animal Care and Use Committee of Union Hospital, Tongji Medical College, Huazhong University of Science and Technology, Wuhan 430022, China ([2023] Institutional Animal Care and Use Committee Number: 3829). All the animal experiments were performed following the Guidelines for Care and Use of Laboratory Animals of Huazhong University of Science and Technology.

Expression Analyses of CD24 Protein and Siglec-10 in Residual Human HCC Samples After RFA

To explore the expression difference of CD24 in normal liver tissues between HCC tissues, the RNA-sequencing data of liver cancer patients (TCGA-LIHC cohort) were obtained from the cancer genome atlas (TCGA) database (https://portal.gdc.cancer.gov/). R Foundation for Statistical Computing software (Version 4.3.1, Vienna, Austria) was used to sort out these data. The expression files for the probes were downloaded from the genomic data commons portal and then mapped to gene names using the Ensembl database. Eventually, the expression of CD24 in 419 samples from the TCGA database was selected for plotting in this analysis, in which 50 samples were from normal liver tissues and 369 samples from the HCC tissues.

To explore the expressions of CD24 and Siglec-10 in residual HCC after iRFA treatment, three non-treated HCC samples from three different patients and three human residual tumors samples after iRFA of HCC from three different patients were harvested by surgical resection, and the CD24 protein and Siglec-10 expressions in the samples of non-treated HCCs and residual HCCs were immunohistochemically assessed. The experiments on human HCC tissues were conducted in accordance with the guiding principles of the Declaration of Helsinki and were approved by the medical ethics committee of Union Hospital, Tongji Medical College, Huazhong University of Science and Technology (No: IEC-20240821). A written informed consent was obtained from all patients before analyzing their HCC samples.

In-vitro Experiments Exploring the Effect of Radiofrequency Hyperthermia (RFH) in Combination with Knocking-Out of CD24 on hepa1-6 Cells

TAMs Extraction, and CD24 Protein and Siglec-10 Expression Analyses

The hepa1-6 cells (1×10^6) were subcutaneously injected into the right thigh of the C57BL/6 mice. When the maximum tumor diameter reached 6–8 mm, the tumors were harvested, and then were made into single-cell suspension with trypsin and collagenase. The TAMs in the tumors were extracted for in-vitro cell experiments through at least three rounds of magnetic activated cell sorting (MACS) (MicroBeads: mouse Anti-F4/80 MicroBeads UltraPure, No. 130–110-443, Miltenyi Biotec, Germany). The expressions of CD24 protein in hepa1-6 cells and Siglec-10 in TAMs were determined after an RFH at 42°C with or without CD24 knocking-out. Samples were divided into three groups: (1) TAMs+hepa1-6 group: TAMs (1×10^5) were co-cultured with hepa1-6 cells (1×10^6) for 48 hours; (2) TAMs+hepa1-6+RFH group: TAMs were co-cultured with hepa1-6 cells, and an RFH was performed at 42°C for 30 minutes, and then the cells were cultured for 48 hours; (3) TAMs+CD24-KO-hepa1-6+RFH group: TAMs were co-cultured with CD24 knocked-out hepa1-6 cells, an RFH was conducted at 42°C for 30 minutes, and then the cells were cultured for 48 hours. The RFH was performed as previously described.[32,33] Briefly, the RFH was performed by placing a 0.022-inch magnetic resonance imaging heating guidewire under the bottom of chamber four of the chamber slides. A fiber optical temperature probe (400-μm, PhotonControl, Burnaby, British Columbia, Canada) was placed in the chamber for temperature measurement. The temperature was kept at 42°C via adjusting radiofrequency output power at about 30 W. After 48 hours of co-culture, the co-culture mixtures in the three groups were collected for Western blotting to assess the CD24 protein and Siglec-10 expressions in the three groups. Meanwhile, a quantitative real-time polymerase chain reaction (qRT-PCR) was performed to measure the mRNA levels of CD24 and Siglec-10 in the three groups. The Western blot assay and qRT-

PCR assay are described in the Supplemental Materials and Methods. The antibodies used in the Western blot are listed in Supplemental Table 1, and the sequences of the primers for qPCR analysis are given in Supplemental Table 2.

In-vitro Evaluation of the Phagocytic Ability of TAMs

To assess the phagocytic ability of TAMs, the GFP-positive hepa1-6 cells instead of the hepa1-6 cells in the aforementioned three groups were stained to label the TAMs. The labelled TAMs were then examined by flow cytometry, scanning electron microscopy (SEM, Hitachi Regulus 8100), and transmission electron microscopy (TEM, Hitachi HT7700). The protocols of flow cytometry are described in the Supplemental Materials and Methods.

Cell Migration Assay and Transwell Migration Assay

The invasion of hepa1-6 cells after RFH plus CD24 knocking-out was assessed in the following three groups: (1) control group: hepa1-6 cells were cultured for 48 hours; (2) RFH group: hepa1-6 cells received an RFH treatment at 42°C for 30 minutes, and then were cultured for 48 hours; (3) RFH+CD24 knocking-out (CD24-KO) group: the CD24 knocked-out hepa1-6 cells were subjected to an RFH treatment at 42°C for 30 minutes, and then cultured for 48 hours. Afterwards, the cell migration assay and transwell migration assay,[34] which were detailed in the Supplemental Materials and Methods, were performed to assess the invasion of hepa1-6 cells with different treatments.

In-vivo Assessment of the Effect of iRFA on Orthotopic hepa1-6 Tumors with CD24 Knocked-out

Tumor Treatments

Under anesthesia with 1–3% isoflurane (RWD Life Science Co., Ltd, Shenzhen, China) delivered in the inhalation of 100% oxygen, the mouse orthotopic HCC models and orthotopic HCC iRFA models were created as described in our previous studies.[27,35] For creating the orthotopic HCC iRFA models, the electrode was inserted into the tumor from the edge of tumor under ultrasound imaging guidance, and ablation was performed at a power output of 70°C for two minutes. This protocol can result in about 70% tumor necrosis and 30% residual viable tumors, which was confirmed by hematoxylin and eosin (H&E) staining in our previous study.[35] The mice orthotopic HCC models were randomly divided into three groups (six mice per group): (1) control group: a pseudo iRFA, with which the ablation electrode was only put in the live tumor but without ablation, was performed; (2) iRFA group: the orthotopic hepa1-6 tumors of mouse only received iRFA alone; (3) iRFA+CD24-KO group: the orthotopic mouse hepa1-6 tumors with CD24 knocked-out received iRFA treatment. The ultrasound imaging was used to observe the tumor growth of mice and quantitatively measure the change in tumor size. The tumor volume was calculated by using the equation of $v= \pi \cdot x \cdot y \cdot z/6$, where v represents the volume of tumors, y refers to the axial diameter of liver tumors, x indicates the longitudinal diameter of liver tumors, and z means the depth diameter of liver tumors. The mice survival time in each group was evaluated from the day of initial treatment and was monitored for 60 days. If the maximum tumor diameter was observed over 2-cm or the mice were found to be moribund during the treatment period, the mice were euthanized. The time point of euthanasia was recorded as the time point of mouse death.

Flow Cytometrical Analysis of Treated Tumors

The mice were euthanized 21 days after treatment. Tumors in each group were collected from mice liver and then weighted and were prepared into single-cell suspension with trypsin and collagenase. For further analysis, the single-cell suspension was filtered via a cell mesh, and was stored in Hank's medium, which was added 1% fetal calf serum (FCS). Antibodies against CD24, Siglec-10, CD206, CD86, CD45, CD3, CD4, NK1.1, CD8, TNF-α, IFN-γ, Foxp3, CD11c, CD11b, F4/80, and GR1 (BD Biosciences, CA, USA) were used for flow cytometrical analysis. To stain intracellular TNF-α and IFN-γ, the cells were stimulated with ionomycin (500 ng/mL) and PMA (50 ng/mL) for 4 hours. Subsequently, the cells were incubated with brefeldin A (10 μg/mL) for 1 hour. Then, the cells were permeabilized by using a permeabilization kit and a Foxp3 fixation (eBioscience, CA, USA), and stained with IFN-γ and TNF-α according to the manufacturer's protocols. For intracellular staining, the cells were permeabilized with a permeabilization kit and a FoxP3 fixation, and then stained for Foxp3. Subsequently, the stained cells were flow cytometrically analyzed and the

data were analyzed by employing a flow Jo software package (Tree Star, Ashland, OR). The detailed gating strategy was provided in Figure S1.

Enzyme-Linked Immunosorbent Assay (ELISA) of Cytokines in the Peripheral Blood of Treated Mice

At 21 days after treatment, the peripheral blood of treated mice was collected via the tail vein into tubes containing Ethylene Diamine Tetraacetic Acid (EDTA). The plasma was obtained by centrifugation at 1000 g for 10 minutes and stored at −80°C until analysis. The concentrations of IFN-γ, TNF-α, CCL2, IL-10, IL-4, TGF-β in the plasma were measured by ELISA kits (Biosciences, California).

In-vivo Assessment of the Feasibility of Using Anti-CD24 Antibody Plus L-Dox for Removal of Residual Tumors After iRFA of HCC

Tumor Treatments, Flow Cytometrical Analysis of the Treated Tumors, and ELISA for Cytokines in Peripheral Blood

The mice orthotopic HCC models were randomly divided into five groups (six per group): (1) control group: a pseudo iRFA, by which the ablation electrode was just put in the live tumor but without ablation treatment, was performed; (2) iRFA group: tumors received iRFA treatment alone; (3) iRFA+anti-CD24 antibody group: tumors were subjected to iRFA, followed by intraperitoneal injection of anti-CD24 antibody (50 μg at day 0, and 200 μg at days 2, 4, 6 after treatment, clone SN3, Creative Diagnostics, New York) in 100 μL phosphate buffered saline (PBS); (4) iRFA+L-Dox group: tumors were treated with iRFA, immediately followed by intratumorally injecting L-Dox (1 mg/kg, size: 100 nm, encapsulation efficiency: 99%, molecular weight: 579.99, zeta potential: 0~-20mV, CSPC Pharmaceutical Group Limited, Shijiazhuang, China, Supplemental Table 3); (5) iRFA+anti-CD24 antibody+L-Dox group: tumors received iRFA treatment, and then injected anti-CD24 antibody intraperitoneally (50 μg at day 0, and 200 μg at days 2, 4, 6 after initial treatment, clone SN3, Creative Diagnostics, New York) in 100 μL PBS, and then L-Dox intratumorally (1 mg/kg) immediately after iRFA. The ultrasound imaging was used to observe the tumor growth and quantitatively determine the tumor size. The tumor volume, tumor weight, and the mice survival were assessed. Since the tumors in the iRFA+CD24 +L-Dox group may significantly regress at 21 days after treatment, the tumors analysis was performed at day 14 after treatments. The improvement of the immune microenvironment of the treated tumor was analyzed by the flow cytometry. At day 21 after treatment, the peripheral blood of treated mice was collected via the mice tail vein, and ELISA was conducted to assess cytokine levels in the peripheral blood of mice.

Histopathological Analysis

At day 14 after treatment, the treated mice were euthanized, and the tumors of mice were taken for histopathological examination. The tumors were fixed with paraformaldehyde (4%), paraffin-embedded, and cut into slices at 4-μm thickness. Six histopathological sections were examined for each tumor. Tissue sections of tumors were stained with CD24, Siglec-10, Foxp3, NKp44, CD4, CD8, Ki-67, terminal deoxynucleotidyl transferase dUTP nick end labeling (TUNEL).

Rechallenge Test and Abscopal Effect Test

To assess the abscopal effect of CD24 antibody plus L-Dox for residual tumors, the hepa1-6 cells (5×10^6) were subcutaneously injected into the right thigh of orthotopic HCC-bearing mice. When the size of tumor in right thigh of mice reached approximately 100 mm^3, the corresponding treatments against orthotopic HCC of mice were initiated. At 21 days after treatments, the treated mice were euthanized, the spleens of mice were obtained and stained with antibodies of anti-CD3, anti-CD8, and anti-CD44 (BD Biosciences), and then a flow cytometry was performed to detect the immune memory cells ($CD8^+CD44^+$ T cells) in the spleen.

In the re-challenge test, the corresponding treatments against orthotopic tumors were discontinued six days after treatments. The age-matched healthy mice, which survived for 30 days after initial treatments, were injected subcutaneously with hepa1-6 cells (1×10^6) in 100-μL PBS into the right thigh. The size of subcutaneous tumors was recorded by ultrasound imaging every three days, and the tumor volume was calculated.

Safety Assessment

At 21 days after treatments, the treated mice were euthanized, and the heart, normal liver, spleen, lungs, and kidneys of the mice were obtained and stained with H&E. Meanwhile, the fixed sections from iRFA+anti-CD24 antibody+L-Dox group were stained with 4',6-Diamidino-2'-phenylindole (DAPI) to observe the distribution of L-Dox in the main organs with fluorescent microscopy. Additionally, the blood biochemical parameters of treated mice, such as glutamic pyruvic transaminase (ALT), glutamic oxaloacetic transaminase (AST), creatine kinase (CK), and creatinine (CREA), were measured.

Statistical Analysis

In this study, the GraphPad Prism (Version 8.0, GraphPad Software, San Diego, California) and SPSS 24.0 software (SPSS Inc, Chicago, IL) were used for statistical analyses. The data between or among different groups were compared by two-sample *t*-test, one-way analysis of variance (ANOVA), or Kruskal-Walli's test. The mice overall survival (OS) in each treated group was analyzed with the Kaplan-Meier method and compared by Log rank test. A two tailed *p*-value less than 0.05 was considered statistically significant.

Results

CD24 and Siglec-10 Expression in Residual HCCs

The bioinformatic analysis demonstrated that expression of CD24 protein was significantly stronger in human HCCs than in the human normal liver ($p<0.001$, Figure 1A). The immunohistochemical staining showed that the expression levels of CD24 protein and Siglec-10 were significantly higher in the residual HCC than in the non-treated HCC ($p<0.001$, Figure 1B–D).

The Effect of RFH in Combination with CD24 Knocking-Out on hepa1-6 Cells

The Western blotting assay showed a sublethal RFH treatment significantly increased the expression of CD24 in hepa1-6 cells and expression of Siglec-10 in TAMs. However, these expressions were significantly decreased when the CD24 gene of hepa1-6 cells was knocked out ($p<0.001$, Figure 1E and F). The qRT-PCR assay showed a sublethal RFH treatment significantly increased the mRNA levels of CD24 and Siglec-10, but they were significantly decreased by CD24 knocking-out treatment ($p<0.001$, Figure 1G and H). These results confirmed that a sublethal RFH in combination with CD24 knocking-out treatment could significantly decrease the expression of CD24 in hepa1-6 cells and expression of Siglec-10 in TAMs.

The transwell migration assay and cell migration assay demonstrated a sublethal RFH significantly enhanced the invasion of hepa1-6 cells, and the effect was significantly reversed by knocking out CD24 of hepa1-6 cells ($p<0.001$, Figure 1I–L). The flow cytometry analysis indicated a sublethal RFH treatment significantly weakened the phagocytotic ability of TAMs, but a sublethal RFH in combination with knocking out CD24 of hepa1-6 cells significantly enhanced the phagocytotic ability of TAMs ($p<0.001$), which were confirmed by the scanning electron microscopy (SEM) and transmission electron microscopy (TEM) (Figure 2A–C). Taken together, these results demonstrated a sublethal RFH treatment can significantly enhance the invasion of hepa1-6 cells and weakened the phagocytotic ability of TAMs, which could be significantly reversed by CD24 knocking-out treatment.

The Effect of iRFA on CD24 Knocked-out hepa1-6 Tumors

Creation of Orthotopic HCC Models in Mice

The mice orthotopic HCC was observed in the left lobe of liver 14 days after tumor implantation in the iRFA and control groups, and 18 days after tumor implantation in the iRFA+CD24-KO group. The tumor volume at baseline in the three groups measured 120.4 mm^3 ± 14.35, 120.9 mm^3 ± 14.5, 119.9 mm^3 ± 14.4, respectively, with no statistically significant differences among them ($p=0.997$).

Assessment of the Treatment Effect

At day 21 after treatments, among the three groups, the smallest tumor volume was observed in the iRFA+CD24-KO group, with the tumor volume in the three groups at day after treatment measured 827.3 mm^3 ± 22.5, 1058.7 mm^3 ± 26.4,

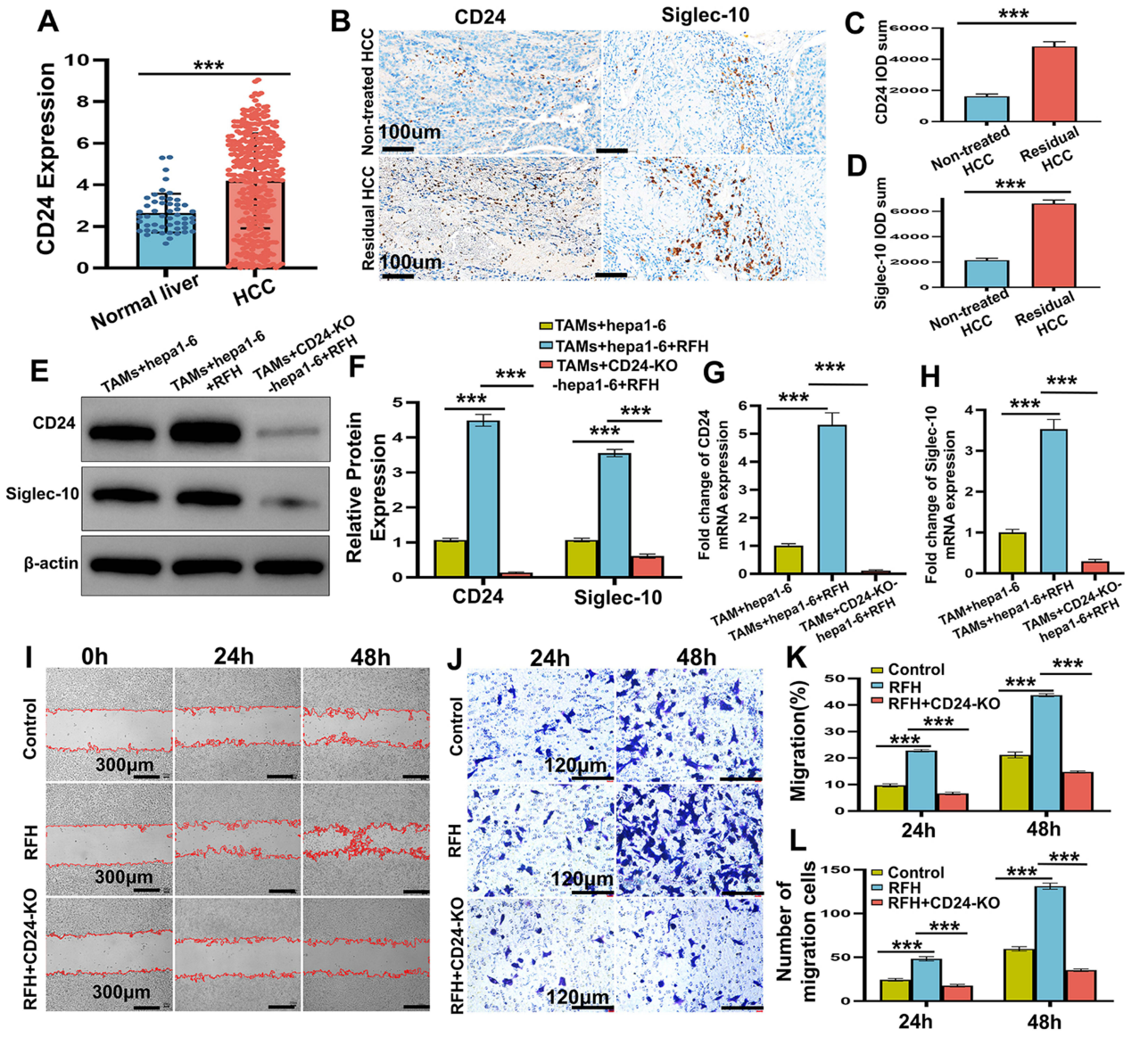

Figure 1 Expressions of CD24 and Siglec-10 in residual HCC after incomplete radiofrequency ablation, and the effect of RFH plus CD24 knocking-out on hepa1-6 cells in vitro. (**A**) The bioinformatic analysis showed CD24 was highly expressed in human HCC. (**B**–**D**) The immunohistochemical staining of human HCC samples exhibited the expression levels of CD24 and Siglec-10 were significantly higher in residual HCC than in the non-treated HCCs. (**E**–**H**) The Western blotting and qRT-PCR demonstrated that a sublethal RFH could significantly increase the expressions of CD24 and Siglec-10, and these expressions could be significantly decreased by knocking out CD24 in hepa1-6 cells. (**I**–**L**) The cell migration and transwell assays showed RFH+CD24-KO group had the fewest migrating cells. ***$p<0.001$. All the data are presented as the mean ± standard deviation. Two-sample *t*-test. Kruskal-Walli's test (n=3). Error bars represent standard deviation.

Abbreviations: Siglec-10, sialic-acid-binding Ig-like lectin 10; HCC, hepatocellular carcinoma; RFH, radiofrequency hyperthermia; qRT-PCR, quantitative real-time polymerase chain reaction; SEM, scanning electron microscopy; TEM, transmission electron microscopy; TAMs, tumor-associated macrophages; CD24-KO, CD24 knocking out; CD24-KO-hepa1-6 cells, CD24 knocked out hepa1-6 cells.

85.3 mm^3 ± 20.3 ($p<0.001$, Figure 3A and B). Meanwhile, the tumor weight was lowest in the iRFA+CD24-KO group among the three groups, with the tumor weight in the three groups measured 0.97 g ± 0.05, 1.21 g ± 0.05, 0.11 g ± 0.02 ($p<0.001$, Figure 3C and D). Additionally, the mice in iRFA+CD24-KO group had the heaviest body weight among the three groups ($p<0.001$, Figure S2A). The Kaplan-Meier survival analysis showed the tumor bearing mice in the iRFA +CD24-KO group had the longest survival time, with the median survival time in the three groups observed 24.5 days, 22 days, 60 days ($p<0.001$, Figure 3E). These results demonstrated CD24 knocked-out treatment could inhibit the residual tumors after iRFA of hepa1-6 tumors.

https://doi.org/10.2147/ITT.S539926

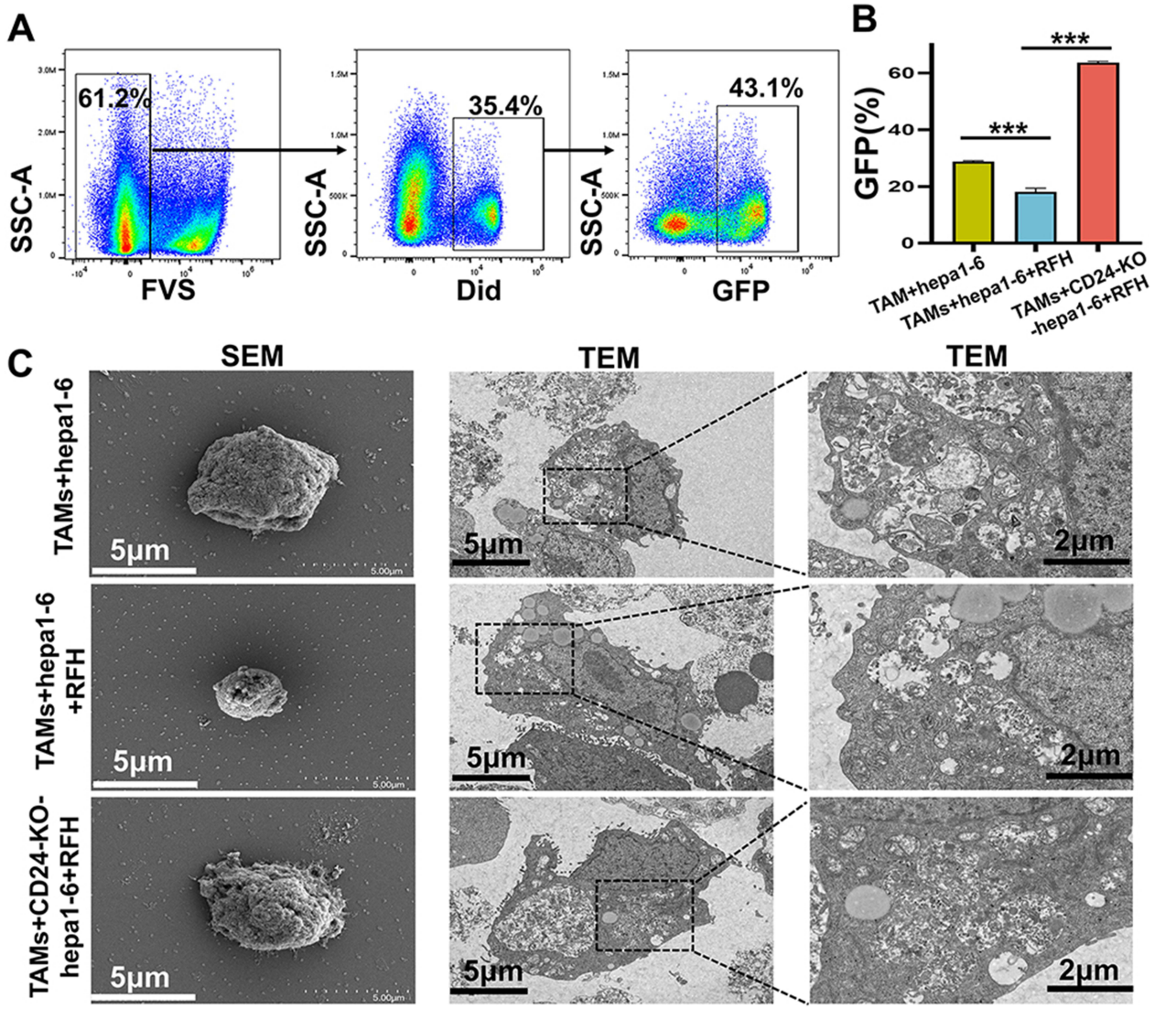

Figure 2 The assessment of phagocytic ability of TAMs after RFH. (**A**–**C**) The flow cytometry, scanning electron microscopy (SEM), and transmission electron microscopy (TEM) indicated the TAM+CD24-KO-hepa1-6+RFH group had the strongest phagocytotic ability of TAMs. All the data are presented as the mean ± standard deviation. Kruskal-Walli's test (n=3), ***p<0.001. Error bars represent standard deviation.

Abbreviations: HCC, hepatocellular carcinoma; RFH, radiofrequency hyperthermia; TAMs, tumor-associated macrophages; CD24-KO, CD24 knocked out; CD24-KO-hepa1-6 cells, CD24 knocking out hepa1-6 cells; GFP, green fluorescent protein.

Immune Microenvironment Analysis of Treated Tumors and ELISA of Cytokines in the Peripheral Blood of Treated Mice

As shown in Figure 4A–L, 21 days after treatments, the flow cytometry revealed a significantly lower expression of CD24 and Siglec-10, a significantly higher percentage of M1-like TAMs, a significantly lower percentage of M2-like TAMs, and significantly higher percentage of NK cells, $CD8^+$T cells, $CD8^+$T/TNF-α^+ T cells, $CD8^+$T/IFN-γ^+ T cells, DC cells, and mature DC cells in the iRFA+CD24-KO group compared to the control group and iRFA group (all p<0.001). Meanwhile, the results showed the iRFA treatment resulted in a significant increase of MDSCs and Tregs in residual tumors (p<0.001), and CD24 knocked-out treatment did not lead to a significant decrease of MDSCs and Tregs in residual tumors (p=0.075, p=0.084). These results demonstrated CD24 knocked-out treatment could enhance the anti-tumor immune microenvironment after iRFA of HCC.

As shown in Figure 4M–R, the ELISA showed that iRFA+CD24-KO group had the highest levels of serum IFN-γ and TNF-β and significantly lower levels of serum CCL2 and IL-4 when compared with the other two groups (all p<0.001).

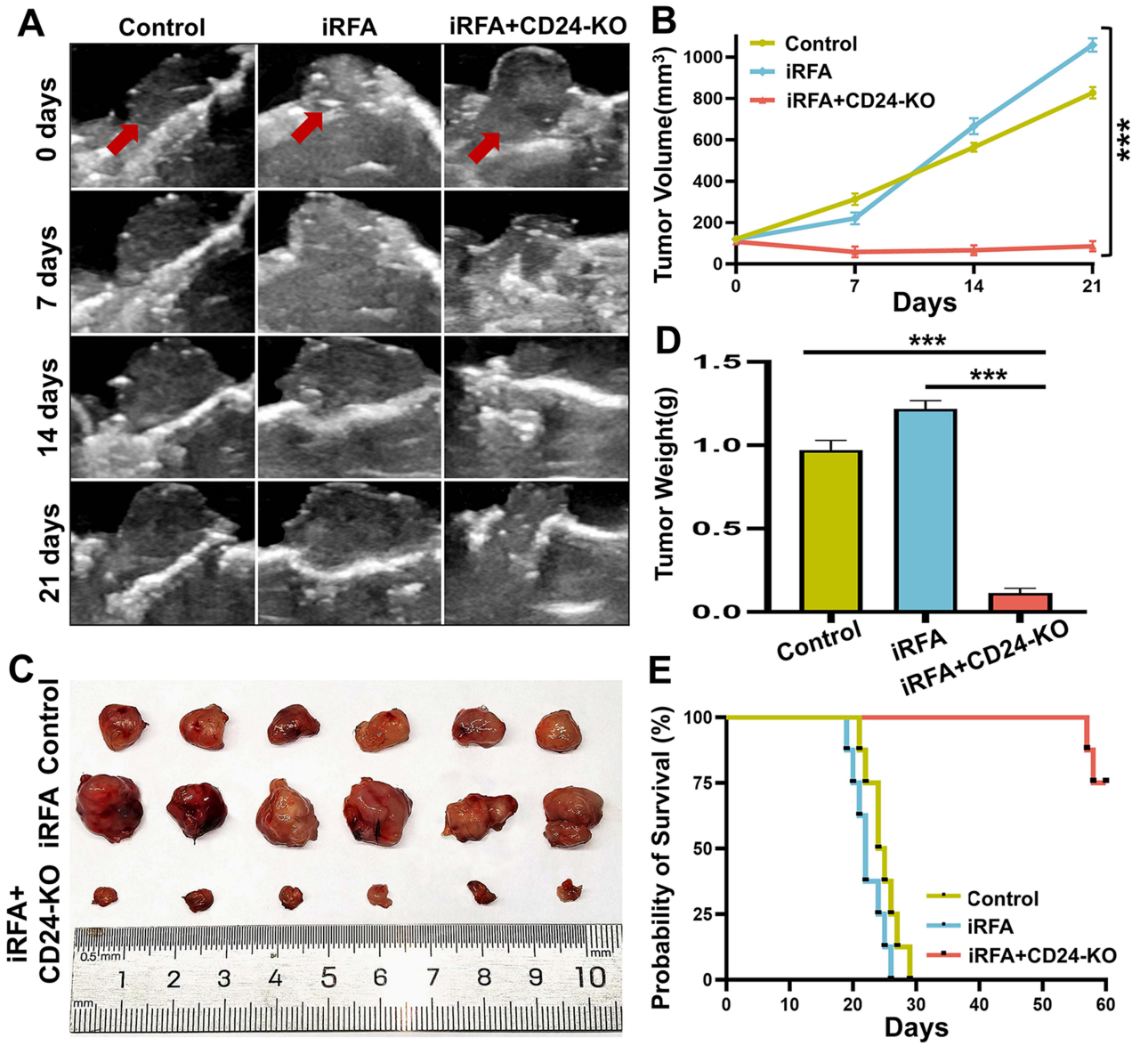

Figure 3 The effect of iRFA on CD24-KO orthotopic hepa1-6 tumors. (**A** and **B**) The ultrasound imaging and quantitative analysis showed the iRFA+CD24-KO group had the smallest tumor (red arrow) volume 21 days after iRFA treatment. (**C** and **D**) iRFA+CD24-KO group had the lowest tumor weight among the three groups at 21 days after iRFA treatment. (**E**) The Kaplan-Meier survival curves showed the tumor bearing mice in the iRFA+CD24-KO group enjoyed the longest survival time. Data are presented as the mean ± standard deviation. One-way ANOVA (n=6), Log rank test. ***$p<0.001$. Error bars represent standard deviation.
Abbreviations: iRFA, incomplete radiofrequency ablation; CD24-KO, CD24 knocked out.

In addition, the levels of serum IL-10 and TGF-β were significantly higher in the iRFA group than in the control group ($p<0.001$), while they were comparable between the iRFA+CD24-KO group and iRFA group ($p=0.071$, $p=0.117$).

The Efficacy and Safety of Anti-CD24 Antibody Plus L-Dox for Residual HCC Tumors After iRFA

Creation of Orthotopic HCC Models in Mice

The mice orthotopic HCCs were found in the left lobe liver 14 days after tumor implantation. The tumor volume at baseline in the five groups was 120.3 mm^3 ± 14.3, 120.2 mm^3 ± 14.7, 121.2 mm^3 ± 14.0, 120.3 mm^3 ± 14.3, 120.5 mm^3 ± 14.3, respectively, with no statistically significant differences among the five groups ($p=0.993$).

https://doi.org/10.2147/ITT.S539926

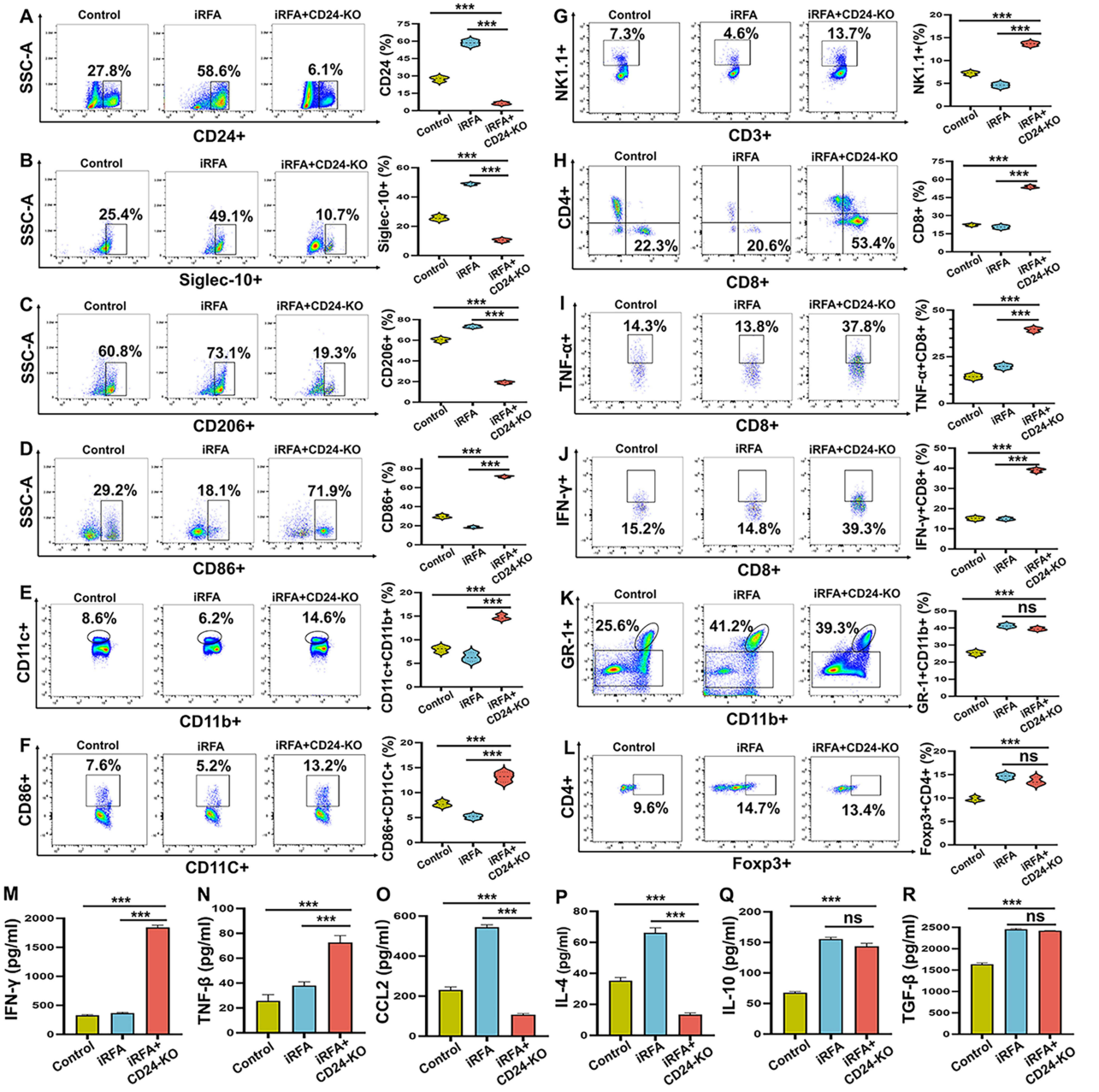

Figure 4 The immune microenvironment of treated tumors and ELISA of cytokine in plasma. The flow cytometric examination of treated tumors and quantitative analysis showed the iRFA+CD24-KO group had the lowest expressions of CD24 (**A**) and Siglec-10 (**B**), the lowest ratio of M2-TAMs (**C**) and the highest ratio of M1-TAMs (**D**), the highest ratios of DCs (**E**) and matured DCs (**F**), and the highest ratios of NK cells (**G**), CD8+T cells (**H**), CD8+T/TNF-α+ T cells (**I**), and CD8+T/IFN-γ+ T cells (**J**). Meanwhile, the ratios of MDSCs and Tregs in the iRFA+CD24-KO group were similar to those in the iRFA group, which were significantly higher than those in the control group (**K** and **L**). The ELISA revealed significantly higher levels of IFN-γ (**M**) and TNF-β (**N**), and significantly lower levels of CCL2 (**O**) and IL-4 (**P**) in the iRFA+CD24-KO group compared to the control or iRFA group. Additionally, the levels of IL-10 and TGF-β in the iRFA+CD24-KO group and iRFA group were comparable, while the levels of IL-10 and TGF-β in the iRFA+CD24-KO group and iRFA group were significantly higher than those in the control group (**Q** and **R**). Data are presented as the mean ± standard deviation. One-way ANOVA (n=6). ***$p<0.001$. ns: no significance. Error bars represent standard deviation.

Abbreviations: ELISA, Enzyme-Linked Immunosorbent Assay; TAMs, tumor-associated macrophages; iRFA, incomplete radiofrequency ablation; Siglec-10, sialic-acid-binding Ig-like lectin 10; NK cells, natural kill cells; DC, dendritic cells; MDSCs, myeloid-derived suppressor cells; Tregs, regulatory T cells.

Assessment of the Treatment Effect

The treatment protocol is described in Figure 5A. The ultrasound imaging showed the tumors completely regressed in the iRFA+anti-CD24 antibody+L-Dox group at 21 days after initial treatment, and the iRFA+anti-CD24 antibody+L-Dox group had the lowest tumor volume among the five groups, with the tumor volume in the five groups at day after

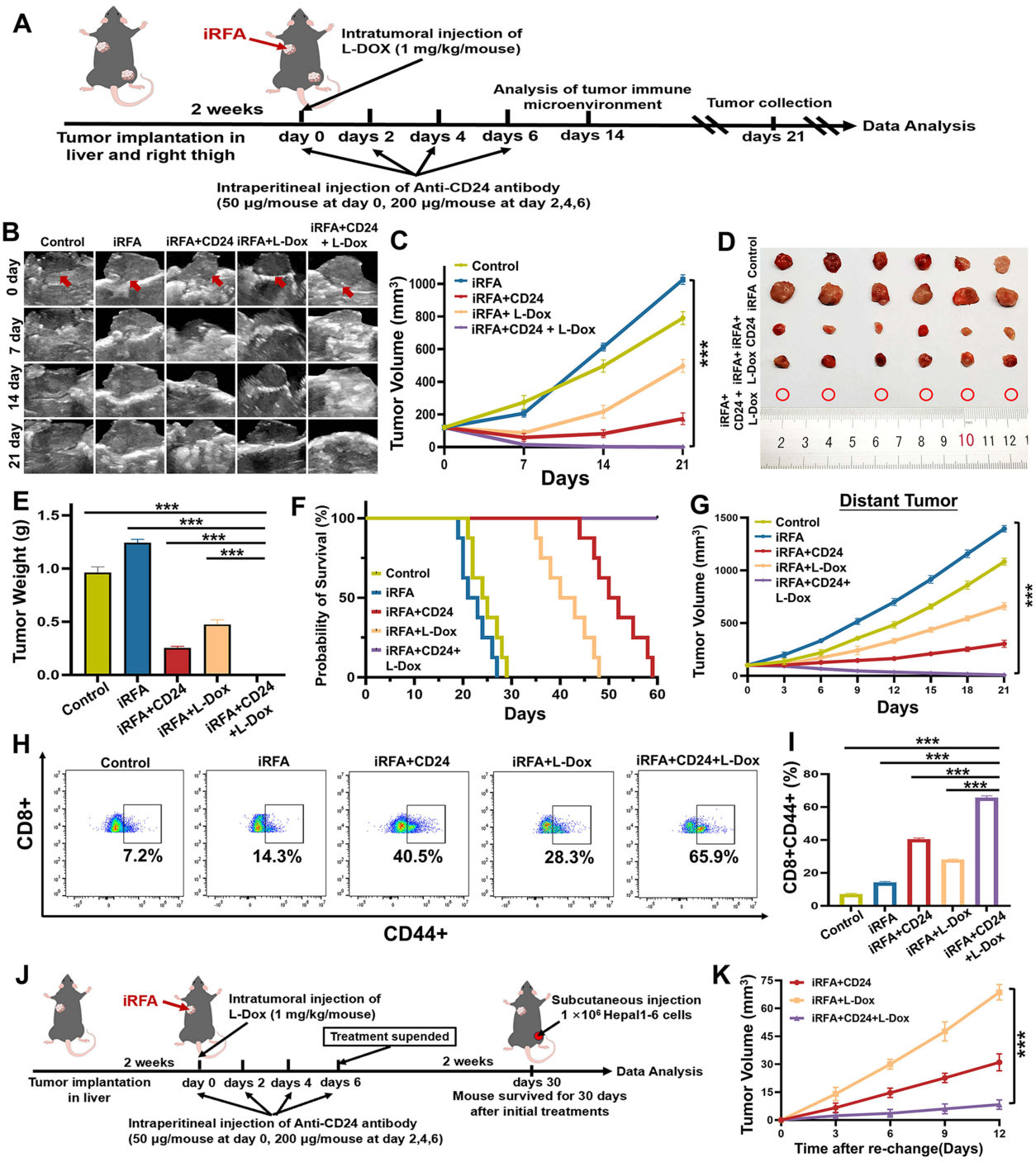

Figure 5 The effect of anti-CD24 antibody plus L-Dox on residual cancers after iRFA of HCC. (**A**) The treatment schedule of anti-CD24 antibody plus L-Dox for residual cancers after iRFA of HCC. (**B** and **C**) The ultrasound imaging showed the tumors completely regressed in the iRFA+anti-CD24 antibody+L-Dox group at 21 days after initial treatment (**B**), and the smallest tumor volume in the iRFA+anti-CD24 antibody+L-Dox group (**C**). (**D** and **E**) The iRFA+anti-CD24 antibody+L-Dox group had the lowest tumor weight among the five groups. (**F**) The Kaplan-Meier survived curves showed the iRFA+anti-CD24 antibody+L-Dox groupthe had the longest survival time. (**G**) The iRFA+anti-CD24 antibody+L-Dox group had the strongest abscopal effect for distant tumor. (**H** and **I**) The flow cytometry and quantitative analyses revealed the highest percentage of immune memory T cells (CD8+CD44+T) in the iRFA+anti-CD24 antibody+L-Dox group. (**J**) The study schedule of the rechallenge test against rechallenged tumors. (**K**) The rechallenge test revealed the iRFA+anti-CD24 antibody+L-Dox group had the smallest tumor volume. Data are presented as the mean ± standard deviation. One-way ANOVA (n=6), Log rank test. ***$p<0.001$. Error bars represent standard deviation.

Abbreviations: L-Dox, liposome doxorubicin; iRFA, incomplete radiofrequency ablation; HCC, hepatocellular carcinoma.

https://doi.org/10.2147/ITT.S539926

treatment measured 790.0 mm^3 ± 32.8, 1025 mm^3 ± 23.8, 173.7 mm^3 ± 29.2, 497.3 mm^3 ± 32.3, 0 mm^3 ($p<0.001$, Figure 5B–D). Meanwhile, the lowest tumor weight was found in the iRFA+anti-CD24 antibody+L-Dox group among the five groups, with the tumor weight in the five groups measured 0.96 g ± 0.05, 1.24 g ± 0.03, 0.25 g ± 0.16, 0.48 mm^3 ± 0.04, 0 g ($p<0.001$, Figure 5E). Additionally, the mice in iRFA+anti-CD24 antibody+L-Dox group had the heaviest body weight among the five groups ($p<0.001$, Figure S2B). The Kaplan-Meier survival analysis demonstrated that the survival time of mice in the iRFA+anti-CD24 antibody+L-Dox group was longest among the five groups, with the median survival time in the five groups observed 24.5 days, 22 days, 51 days, 41.5 days, 60 days ($p<0.001$, Figure 5F). These results showed the combined therapy of anti-CD24 antibody with L-Dox achieved an excellent therapeutic effect on residual tumors after iRFA of HCC.

Rechallenge Test and Abscopal Effect

As described in Figure 5G, the triple combination treatment (iRFA+anti-CD24 antibody+L-Dox) yielded the strongest abscopal effect among the five groups ($p<0.001$). In addition, the flow cytometry showed that the triple combination treatment led to the most $CD8^+CD44^+$ T cells in the spleen compared with the other four treatments ($p<0.001$, Figure 5H and I). Moreover, as described in Figure 5J, the activation of a systemic antitumor immune response by this combination treatment was assessed by using a rechallenge test. At 30 days after initial treatments, there existed no surviving mice in the control group and iRFA group. So, the mice in the iRFA+anti-CD24 antibody group, iRFA +L-Dox group, iRFA+anti-CD24 antibody+L-Dox group (n=6/group) were selected for rechallenge test. The rechallenge test exhibited the strongest suppressive effect on rechallenged tumors in the iRFA+anti-CD24 antibody+L-Dox group compared with the other two groups ($p<0.001$, Figure 5K). These results demonstrated the combined therapy of anti-CD24 antibody with L-Dox for residual tumors after iRFA of HCC could result in a good systemic anti-tumor effect.

Analysis of Immune Microenvironment of Treated Tumors and ELISA of Cytokines

The flow cytometrical analyses of treated liver tumors showed that the iRFA+anti-CD24 antibody+L-Dox group exhibited a lower expression of CD24 and Siglec-10, a higher percentage of M1-like TAMs, a lower percentage of M2-like TAMs, a higher percentage of natural killer (NK) cells, DC cells, mature DC cells, $CD8^+$T cells, CD8+T/TNF-α^+T cells, and $CD8^+$T/IFN-γ^+ T cells, with a lower percentage of MDSCs and Tregs, when compared with the other four treatment groups (all $p<0.001$, Figure 6A–Q). These results demonstrated the combined therapy of anti-CD24 antibody with L-Dox could significantly improve the tumor immune microenvironment of residual tumors.

ELISA showed the highest levels of serum IFN-γ and TNF-β, and the lowest levels of serum IL-4, CCL2, TGF-β, and IL-10 in the iRFA+anti-CD24 antibody+L-Dox group compared with the other four groups (all $p<0.001$, Figure 6R–W).

Immunohistochemical Analysis

The TUNEL staining showed the most apoptotic cells, and the Ki-67 staining indicated the fewest proliferating cells in the iRFA+anti-CD24 antibody+L-Dox group (all $p<0.001$, Figure 7A–C). Meanwhile, the immunohistochemical staining of Siglec-10, CD24, CD4, CD8, NKp44, and Foxp3 confirmed the flow cytometrical findings in treated liver tumors (all $p<0.001$, Figure 7A, D–I).

Safety Evaluation

As demonstrated in Figure 8A–E, the H&E staining showed no conspicuous pathological changes, such as cellular edema or tissue hyperemia in the normal liver, heart, lungs, kidneys, and spleen of mice after the treatments, and the biochemical analyses exhibited normal levels of AST, ALT, CK, and CREA in the iRFA+anti-CD24 antibody +L-Dox group and relatively higher levels of AST and ALT in the iRFA and control groups. Meanwhile, the fluorescent microscopy showed no distribution of doxorubicin in the heart, normal liver tissue, spleen, lungs, and kidney tissues of treated mice in the iRFA+anti-CD24 antibody+L-Dox group. Taken together, these results demonstrated a good safety of anti-CD24 antibody in combination with L-Dox for residual tumors after iRFA of HCC.

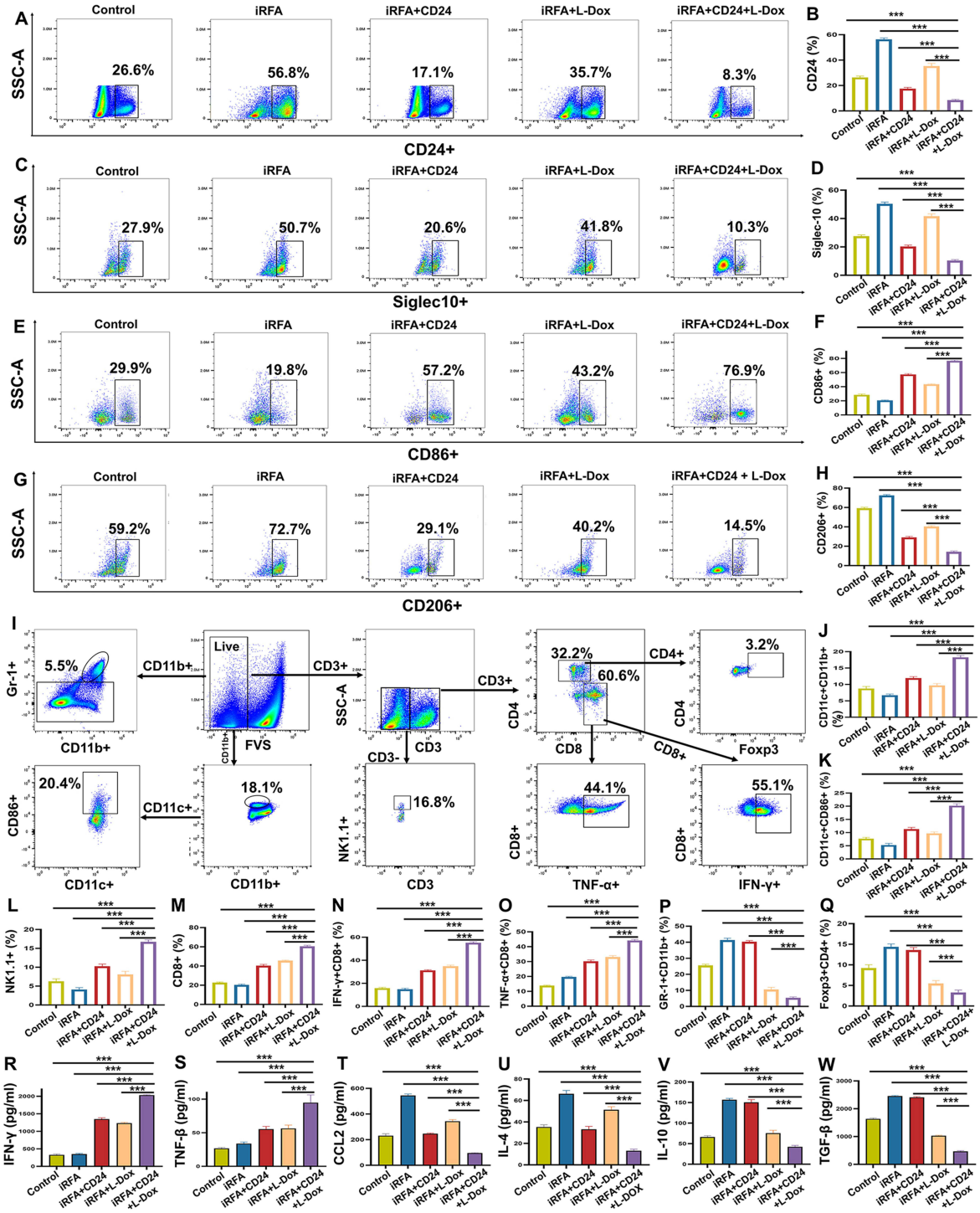

Figure 6 The immune microenvironment of treated tumors among five groups. The flow cytometry showed the lowest expressions of CD24 (**A** and **B**) and Siglec-10 (**C** and **D**), the highest ratio of M1-TAMs (**E** and **F**) and the lowest ratio of M2-TAMs in the iRFA+anti-CD24 antibody+L-Dox group (**G** and **H**). (**I**) The representative dot plots of the morphological characteristics (SSC vs FSC) of tumors subjected to the triple combination treatment (iRFA+anti-CD24 antibody+L-Dox). The flow cytometric and quantitative analyses showed the highest percentages of DCs (**J**), matured DCs (**K**), NK cells (**L**), CD8+T cells (**M**), CD8+T/IFN-γ+ T cells (**N**), CD8+T/TNF-α+ T cells (**O**), and the lowest percentages of MDSCs (**P**) and Tregs (**Q**) in the iRFA+anti-CD24 antibody+L-Dox group. (R-W): The ELISA showed the highest levels of IFN-γ (**R**) and TNF-β (**S**), and the lowest levels of CCL2 (**T**), IL-4 (**U**), IL-10 (**V**), TGF-β (**W**) in the iRFA+anti-CD24 antibody+L-Dox group. Data are presented as the mean ± standard deviation. One-way ANOVA (n=6), Log rank test. ***$p<0.001$. Error bars represent standard deviation.

Abbreviations: ELISA, enzyme-linked immunosorbent assay; Siglec-10, sialic-acid-binding Ig-like lectin; TAM, tumor-associated macrophage; iRFA, incomplete radio-frequency ablation; L-Dox, liposome doxorubicin; NK, natural killer; DCs, dendritic cells; MDSCs, myeloid-derived suppressor cells; Tregs, regulatory T cells.

https://doi.org/10.2147/ITT.S539926

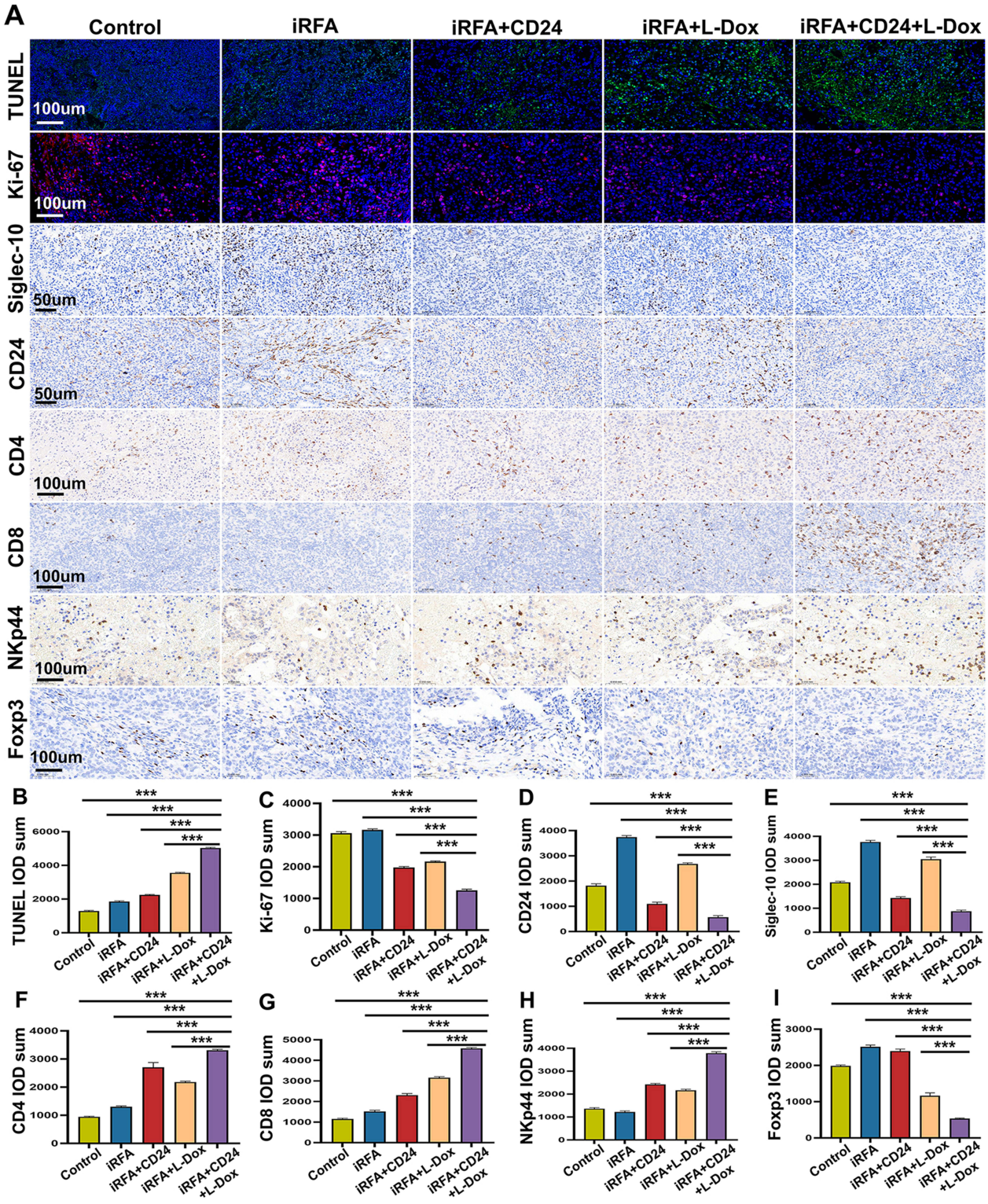

Figure 7 Pathological examination of the treated tumors in the five groups. (**A–I**) The immunohistochemical staining and quantitative analyses showed the most apoptotic cells (green dots), fewest proliferating cells (red dots), lowest expressions of CD24 and Siglec-10, most CD4+T cells, CD8+T cells, and NK cells, and fewest Tregs in the iRFA+anti-CD24 antibody+L-Dox group. Data are presented as the mean ± standard deviation. One-way ANOVA (n=6), Log rank test. ***$p<0.001$. Error bars represent standard deviation.

Abbreviations: Siglec-10, sialic-acid-binding Ig-like lectin; iRFA, incomplete radiofrequency ablation; L-Dox, liposome doxorubicin.

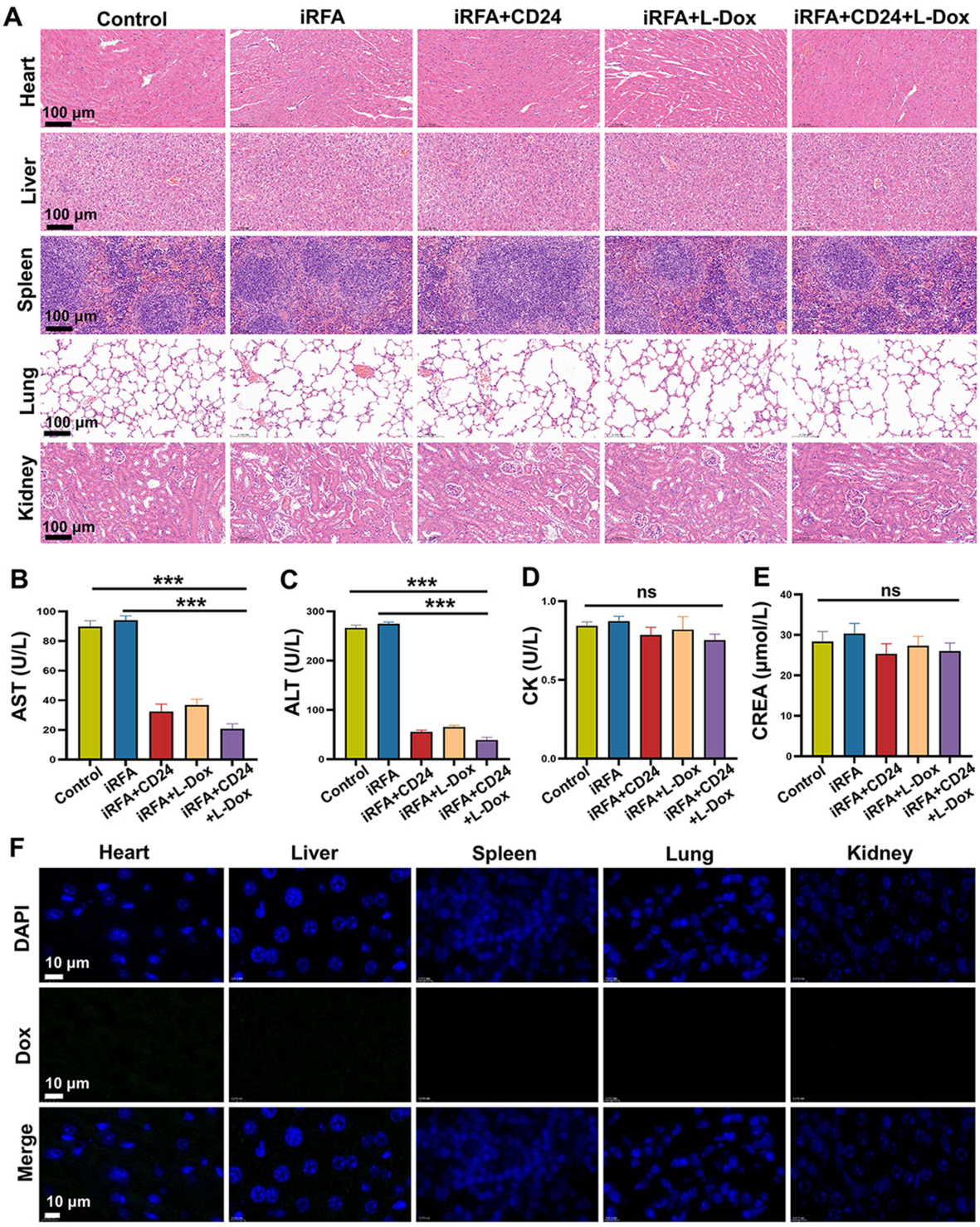

Figure 8 The safety assessment of anti-CD24 antibody plus L-Dox for residual cancers after iRFA of HCC. (**A**) H&E staining for the heart, liver, spleen, lungs, and kidney tissues of treated mice showed no obvious pathological changes in these organs. (**B**–**E**) The biochemical analyses showed normal levels of ALT (**B**), AST (**C**), CK (**D**), and CREA (**E**) in the iRFA+anti-CD24 antibody+L-Dox group. (**F**) The fluorescent microscopy showed no distribution of doxorubicin in the heart, normal liver tissue, spleen, lungs, and kidney tissues of treated mice in the iRFA+anti-CD24 antibody+L-Dox group. Data are presented as the mean ± SD. One-way ANOVA (n=6). ***$p<0.001$. ns: no significance. Error bars represent standard deviation.

Abbreviations: L-Dox, liposome doxorubicin; iRFA, incomplete radiofrequency ablation; HCC, hepatocellular carcinoma; H&E, Hematoxylin and eosin; ALT, glutamic pyruvic transaminase; AST, glutamic oxaloacetic transaminase; CK, creatine kinase; CREA, creatinine.

https://doi.org/10.2147/ITT.S539926

Discussion

Although immunotherapy was proved to be efficatious against HCC, the response rates are still relatively low.[36,37] For instance, a randomized Phase 3 multicenter trial (the CheckMate 459 trial)[38] compared the effect of an immune checkpoint inhibitor (nivolumab) with sorafenib on advanced HCCs, and showed nivolumab failed to significantly improve the overall survival of patients compared with sorafenib, with a low objective response rate (14%) in the nivolumab group. In the present study, we also found that the treatment targeting CD24 alone worked modestly on residual HCC after iRFA. However, the combination of anti-CD24 antibody with liposomal doxorubicin achieved an excellent anti-tumor effect on HCC after iRFA. Therefore, our study provided a new and effective treatment option for lowering the recurrence rate of HCC after RFA, particularly for large sized (>3 cm) HCC or HCC at high-risk locations.

In recent years, some immune checkpoint inhibitors (ICIs) that targeted programmed cell death protein 1 (PD-1)/programmed death ligand 1 (PD-L1), cytotoxic T-lymphocyte-associated protein 4 (CTLA-4) were widely used in the treatment of advanced solid tumors and improved patients' outcomes.[39–41] The main mechanism of these treatments is the regulation of antitumor T cells by immunological checkpoints. Following the discovery of the PD-1/PD-L1 and CTLA-4, a new checkpoint of CD24/Siglec-10 was identified.[19] The CD24/Siglec-10 axis can protect the host against a lethal response to pathological cell death.[42] Targeting the CD24/Siglec-10 axis is emerged as a viable immunotherapy strategy based on the results of some preclinical studies and clinical trials.[19,43,44] In the present study, we found anti-CD24 treatment could improve the immunosuppressive microenvironment of residual tumors. However, it exerted a limited inhibitory effect on Tregs and MDSCs, which may explain the modest effect of the anti-CD24 alone on residual cancers. These results prompted us to use anti-CD24 antibody plus L-Dox for the removal of residual tumors in this study. The findings of our study indicated that anti-CD24 antibody plus L-Dox may be a promising treatment strategy for improving the immunosuppressive microenvironment of solid malignant tumors.

In this study, we found that the combination of anti-CD24 antibody with L-Dox could induce the infiltration of more NK cells and functional $CD8^+$T cells into residual tumors. Meanwhile, the results of abscopal effect experiment and rechallenge test showed this combined therapy could generate a strong anti-tumor immune memory effect. These results suggested that anti-CD24 antibody in combination with L-Dox could elicit a strong local and systemic antitumor immune response, which helps reduce the tumor recurrence and metastasis after RFA of HCC.

The inability to obtain a tumor-free margin is often caused by RFA heat carried away by blood flow when presence of large vasculatures at the peripheral region of tumor (heat-sink effect), which can lead to a sublethal RFH in the residual tumors. The sublethal RFH could further enhanced the effect of immunotherapy and chemotherapy for tumors,[14,32,33] and thereby promoting the tumor destruction. Therefore, the integration of iRFA with the combined use of anti-CD24 antibody and L-Dox may optimize the formation of a tumor-free margin during an RFA procedure for HCC, especially for HCC located adjacent to large vasculatures.

In our study, the safety of anti-CD24 antibody in combination with L-Dox for residual tumors was fully evaluated by H&E staining of the main organs, biochemical analysis of ALT, AST, CK, CERA, and distribution of doxorubicin in the main organs. The results showed that the major organs functioned well and there was no distribution of doxorubicin in the main organs in the iRFA+anti-CD24 antibody+L-Dox group. Moreover, AST and ALT, two measures of hepatic function, were significantly higher in the control and iRFA groups than in the other three groups, which might be ascribed to a greater tumor burden in the control and iRFA groups. These results suggested the strategy of combining anti-CD24 antibody with liposomal doxorubicin was safe for the management of residual tumors after RFA of HCC.

This study has limitations. The reliance on subcutaneous or orthotopic mouse models does not sufficiently reflect the complexity of human HCC, especially in cirrhotic livers or in the presence of hepatitis B or C virus infection. Moreover, although the safety profile of this study was assessed, it was too limited to make claims about the clinical safety.

Conclusion

In conclusion, the combined therapy of anti-CD24 antibody plus L-Dox can reprogram a stronger anti-tumor immune microenvironment of residual tumors after iRFA of HCC, and is effective and safe for managing the residual tumors. Our study may pave the way to lowering HCCs recurrence rate and metastasis after RFA, especially for large-size HCC or

HCC in high-risk locations. The findings and insights of this study could lead to further clinical translation and clinical trials on this treatment application for the management of HCC and polymer engineering technology (eg,co-loaded nanoparticles) to further improve the immune modulation of L-Dox and anti-CD24 antibody for malignant tumors.

Abbreviations

RFA, radiofrequency ablation; L-Dox, liposomal doxorubicin; iRFA, incomplete radiofrequency ablation; HCC, hepatocellular carcinoma; Siglec-10, sialic-acid-binding lg-like lectin 10; TAMs, tumor-associated macrophages; MDSCs, myeloid-derived suppressor cells; GFP, green fluorescent protein; Tregs, regulatory T cells; TCGA, the cancer genome atlas; qRT-PCR, quantitative real-time polymerase chain reaction; NK, natural killer; H&E, hematoxylin and eosin; ELISA, Enzyme-Linked Immunosorbent Assay; PBS, phosphate buffered saline.

Data Sharing Statement

The data of this study are available from the corresponding author on reasonable request.

Declaration of Ethics Approval

The experiment on human HCC samples was approved by the ethics committee of Union Hospital, Tongji Medical College, Huazhong University of Science and Technology, Wuhan 430022, China (No: IEC-20240821). A written informed consent was obtained from all patients before analyzing their HCC samples. The animal experiments of this study were approved by the Animal Use and Care Committee of Union Hospital, Tongji Medical College, Huazhong University of Science and Technology, Wuhan, China ([2023] Institutional Animal Care and Use Committee Number: 3829). All the animal experiments were performed following the Guidelines for Care and Use of Laboratory Animals of Huazhong University of Science and Technology.

Author Contributions

All authors made a significant contribution to the work reported, whether that is in the conception, study design, execution, acquisition of data, analysis and interpretation. All author participated in drafting, revising, or critically reviewing the article. They have all approved the final version of the manuscript for publication, agreed on the choice of journal for submission, and accepted accountability for all aspects of the work.

Funding

This study was supported by the grants of National Natural Science Foundation of China (No. 82372069), Outstanding Youth Foundation of Hubei Province, China (No: 2023AFA107), and National Key R&D Program of China (No. 2024YFC2417805).

Disclosure

The authors declare no competing interests in this work.

References

1. Bray F, Laversanne M, Sung H, et al. Global cancer statistics 2022: GLOBOCAN estimates of incidence and mortality worldwide for 36 cancers in 185 countries. *CA Cancer J Clin*. 2024;74(3):229–263. doi:10.3322/caac.21834
2. European Association for the Study of the Liver. EASL clinical practice guidelines: management of hepatocellular carcinoma. *J Hepatol*. 2018;69 (1):182–236. doi:10.1016/j.jhep.2018.03.019.
3. Zhao Q, Wang J, Fu YL, et al. Radiofrequency ablation for stage <IIB non-small cell lung cancer: opportunities, challenges, and the road ahead. *Thorac Cancer*. 2023;14(32):3181–3190. doi:10.1111/1759-7714.15114
4. Park BK, Shen SH, Fujimori M, et al. Asian conference on tumor ablation guidelines for renal cell carcinoma. *Investig Clin Urol*. 2021;62 (4):378–388. doi:10.4111/icu.20210168
5. Lin ZY, Chen J, Deng XF. Treatment of hepatocellular carcinoma adjacent to large blood vessels using 1.5T MRI-guided percutaneous radio-frequency ablation combined with iodine-125 radioactive seed implantation. *Eur J Radiol*. 2012;81(11):3079–3083. doi:10.1016/j.ejrad.2012.05.007
6. Kan X, Zhang F, Zhou G, et al. Interventional real-time optical imaging guidance for complete tumor ablation. *Proc Natl Acad Sci USA*. 2021;118 (41):e2113028118. doi:10.1073/pnas.2113028118

7. Zhang N, Li H, Qin C, et al. Insufficient radiofrequency ablation promotes the metastasis of residual hepatocellular carcinoma cells via upregulating flotillin proteins. *J Cancer Res Clin Oncol*. 2019;145(4):895–907. doi:10.1007/s00432-019-02852-z
8. Zhang N, Wang LR, Li DD, et al. Interferon-α combined with herbal compound "songyou Yin" effectively inhibits the increased invasiveness and metastasis by insufficient radiofrequency ablation of hepatocellular carcinoma in an animal model. *Integr Cancer Ther*. 2018;17(4):1260–1269. doi:10.1177/1534735418801525
9. Zhang N, Wang L, Chai ZT, et al. Incomplete radiofrequency ablation enhances invasiveness and metastasis of residual cancer of hepatocellular carcinoma cell HCCLM3 via activating β-catenin signaling. *PLoS One*. 2014;9(12):e115949. doi:10.1371/journal.pone.0115949
10. Faraoni EY, O'Brien BJ, Strickland LN, et al. Radiofrequency ablation remodels the tumor microenvironment and promotes neutrophil-mediated abscopal immunomodulation in pancreatic cancer. *Cancer Immunol Res*. 2023;11(1):4–12. doi:10.1158/2326-6066.CIR-22-0379
11. Zerbini A, Pilli M, Penna A, et al. Radiofrequency thermal ablation of hepatocellular carcinoma liver nodules can activate and enhance tumor-specific T-cell responses. *Cancer Res*. 2006;66(2):1139–1146. doi:10.1158/0008-5472.CAN-05-2244
12. Wang K, Wang C, Jiang H, et al. Combination of ablation and immunotherapy for hepatocellular carcinoma: where we are and where to go. *Front Immunol*. 2021;12:792781. doi:10.3389/fimmu.2021.792781
13. Sun B, Zhang Q, Sun T, et al. Radiofrequency hyperthermia enhances the effect of OK-432 for hepatocellular carcinoma by activating of TLR4-cGAS-STING pathway. *Int Immunopharmacol*. 2024;130:111769. doi:10.1016/j.intimp.2024.111769
14. Kan X, Zhou G, Zhang F, et al. Enhanced efficacy of direct immunochemotherapy for hepatic cancer with image-guided intratumoral radiofrequency hyperthermia. *J Immunother Cancer*. 2022;10(11):e005619. doi:10.1136/jitc-2022-005619
15. Shi ZR, Duan YX, Cui F, et al. Integrated proteogenomic characterization reveals an imbalanced hepatocellular carcinoma microenvironment after incomplete radiofrequency ablation. *J Exp Clin Cancer Res*. 2023;42(1):133. doi:10.1186/s13046-023-02716-y
16. Fang Y, Hu F, Ren W, et al. Nanomedicine-unlocked radiofrequency dynamic therapy dampens incomplete radiofrequency ablation-arised immunosuppression to suppress cancer relapse. *Biomaterials*. 2025;317:123087. doi:10.1016/j.biomaterials.2025.123087
17. Yang XR, Xu Y, Yu B, et al. CD24 is a novel predictor for poor prognosis of hepatocellular carcinoma after surgery. *Clin Cancer Res*. 2009;15(17):5518–5527. doi:10.1158/1078-0432.CCR-09-0151
18. Wan X, Cheng C, Shao Q, et al. CD24 promotes HCC progression via triggering notch-related EMT and modulation of tumor microenvironment. *Tumour Biol*. 2016;37(5):6073–6084. doi:10.1007/s13277-015-4442-7
19. Barkal AA, Brewer RE, Markovic M, et al. CD24 signalling through macrophage siglec-10 is a target for cancer immunotherapy. *Nature*. 2019;572(7769):392–396. doi:10.1038/s41586-019-1456-0
20. Cheng K, Cai N, Zhu J, Yang X, Liang H, Zhang W. Tumor-associated macrophages in liver cancer: from mechanisms to therapy. *Cancer Commun*. 2022;42(11):1112–1140. doi:10.1002/cac2.12345
21. Yin SS, Gao FH. Molecular mechanism of tumor cell immune escape mediated by CD24/siglec-10. *Front Immunol*. 2020;11:1324. doi:10.3389/fimmu.2020.01324
22. Vitale I, Manic G, Coussens LM, Kroemer G, Galluzzi L. Macrophages and metabolism in the tumor microenvironment. *Cell Metab*. 2019;30(1):36–50. doi:10.1016/j.cmet.2019.06.001
23. Wang Y, Yu H, Yu M, et al. CD24 blockade as a novel strategy for cancer treatment. *Int Immunopharmacol*. 2023;121:11055. doi:10.1016/j.intimp.2023.110557
24. Altevogt P, Sammar M, Hüser L, et al. Novel insights into the function of CD24: a driving force in cancer. *Int J Cancer*. 2021;148(3):546–559. doi:10.1002/ijc.33249
25. Makwana V, Karanjia J, Haselhorst T, Anoopkumar-Dukie S, Rudrawar S. Liposomal doxorubicin as targeted delivery platform: current trends in surface functionalization.Int. *J Pharm*. 2021;593:120117. doi:10.1016/j.ijpharm.2020.120117
26. Li TF, Xu YH, Li K, et al. Doxorubicin-polyglycerol-nanodiamond composites stimulate glioblastoma cell immunogenicity through activation of autophagy. *Acta Biomater*. 2019;86:381–394. doi:10.1016/j.actbio.2019.01.020
27. Cao Y, Sun T, Sun B, et al. Injectable hydrogel loaded with lysed OK-432 and doxorubicin for residual liver cancer after incomplete radiofrequency ablation. *J Nanobiotechnology*. 2023;21(1):404. doi:10.1186/s12951-023-02170-0
28. Chen Y, Qin H, Li N, et al. Neoadjuvant chemotherapy by liposomal doxorubicin boosts immune protection of tumor membrane antigens-based nanovaccine. *Cell Rep Med*. 2025;6(1):101877. doi:10.1016/j.xcrm.2024.101877
29. Hannesdóttir L, Tymoszuk P, Parajuli N, et al. Lapatinib and doxorubicin enhance the stat1-dependent antitumor immune response. *Eur J Immunol*. 2013;43(10):2718–2729. doi:10.1002/eji.201242505
30. Meng X, Zhang H, Chen L, et al. Liposomal doxorubicin: the sphingomyelin/cholesterol system significantly enhances the antitumor efficacy of doxorubicin. *AAPS PharmSciTech*. 2023;24(2):64. doi:10.1208/s12249-022-02489-1
31. Xu HZ, Li TF, Wang C, et al. Synergy of nanodiamond-doxorubicin conjugates and PD-L1 blockade effectively turns tumor-associated macrophages against tumor cell. *J Nanobiotechnol*. 2021;19(1):268. doi:10.1186/s12951-021-01017-w
32. Shi Y, Zhang F, Bai Z, et al. Orthotopic esophageal cancers: intraesophageal hyperthermia-enhanced direct chemotherapy in rats. *Radiology*. 2017;282(1):103–112. doi:10.1148/radiol.2016152281
33. Song J, Zhang F, Ji J, et al. Orthotopic hepatocellular carcinoma: molecular imaging-monitored intratumoral hyperthermia-enhanced direct oncolytic virotherapy. *Int J Hyperthermia*. 2019;36(1):344–350. doi:10.1080/02656736.2019.1569731
34. Armartmuntree N, Murata M, Techasen A, et al. Prolonged oxidative stress down-regulates Early B cell factor 1 with inhibition of its tumor suppressive function against cholangiocarcinoma genesis. *Redox Biol*. 2018;14:637–644. doi:10.1016/j.redox.2017.11.011
35. Sun T, Sun B, Cao Y, et al. Synergistic effect of OK-432 in combination with an anti-PD-1 antibody for residual tumors after radiofrequency ablation of hepatocellular carcinoma. *Biomed Pharmacother*. 2023;166:115351. doi:10.1016/j.biopha.2023.115351
36. Llovet JM, Castet F, Heikenwalder M, et al. Immunotherapies for hepatocellular carcinoma. *Nat Rev Clin Oncol*. 2022;19(3):151–172. doi:10.1038/s41571-021-00573-2
37. Shen KY, Zhu Y, Xie SZ, et al. Immunosuppressive tumor microenvironment and immunotherapy of hepatocellular carcinoma: current status and prospectives. *J Hematol Oncol*. 2024;17(1):25. doi:10.1186/s13045-024-01549-2
38. Yau T, Park JW, Finn RS, et al. Nivolumab versus sorafenib in advanced hepatocellular carcinoma (checkmate 459): a randomised, multicentre, open-label, phase 3 trial. *Lancet Oncol*. 2022;23(1):77–90. doi:10.1016/S1470-2045(21)00604-5

39. Qin S, Chen M, Cheng AL, et al. Atezolizumab plus bevacizumab versus active surveillance in patients with resected or ablated high-risk hepatocellular carcinoma (IMbrave050): a randomised, open-label, multicentre, phase 3 trial. *Lancet*. 2023;402(10415):1835–1847. doi:10.1016/S0140-6736(23)01796-8
40. Voorwerk L, Slagter M, Horlings HM, et al. Immune induction strategies in metastatic triple-negative breast cancer to enhance the sensitivity to PD-1 blockade: the TONIC trial. *Nat Med*. 2019;25(6):920–928. doi:10.1038/s41591-019-0432-4
41. Gao X, Xu N, Li Z, et al. Safety and antitumour activity of cadonilimab, an anti-PD-1/CTLA-4 bispecific antibody, for patients with advanced solid tumours (COMPASSION-03): a multicentre, open-label, phase 1b/2 trial. *Lancet Oncol*. 2023;24(10):1134–1146. doi:10.1016/S1470-2045(23)00411-4
42. Chen GY, Tang J, Zheng P, Liu Y. CD24 and Siglec-10 selectively repress tissue damage-induced immune responses. *Science*. 2009;323(5922):1722–1725. doi:10.1126/science.1168988
43. Shen W, Shi P, Dong Q, et al. Discovery of a novel dual-targeting D-peptide to block CD24/siglec-10 and PD-1/PD-L1 interaction and synergize with radiotherapy for cancer immunotherapy. *J Immunother Cancer*. 2023;11(6):e007068. doi:10.1136/jitc-2023-007068
44. Yang Y, Wu H, Yang Y, et al. Dual blockade of CD47 and CD24 signaling using a novel bispecific antibody fusion protein enhances macrophage immunotherapy. *Mol Ther Oncolytics*. 2023;31:100747. doi:10.1016/j.omto.2023.100747